

## Magnetism and Electronic Correlations in Quasi-One-Dimensional Compounds

M. D. Coutinho-Filho,<sup>1</sup> R. R. Montenegro-Filho,<sup>2</sup> and E. P. Raposo<sup>2</sup>  
 Laboratório de Física Teórica e Computacional, Departamento de Física,  
 Universidade Federal de Pernambuco, 50670-901, Recife-PE, Brazil

C. Vitoriano<sup>3</sup>

Universidade Federal Rural de Pernambuco, Unidade Acadêmica de Garanhuns, 55296-190, Garanhuns-PE, Brazil

M. H. Oliveira<sup>4</sup>

Universidade Federal Rural de Pernambuco, Unidade Acadêmica de Serra Talhada, 56900-000, Serra Talhada-PE, Brazil

(Dated: February 20, 2024)

In this contribution on the celebration of the 80th birthday anniversary of Prof. Ricardo Ferreira, we present a brief survey on the magnetism of quasi-one-dimensional compounds. This has been a research area of intense activity particularly since the first experimental announcements of magnetism in organic and organometallic polymers in the mid 80's. We review experimental and theoretical achievements on the field, featuring chain systems of correlated electrons in a special  $AB_2$  unit cell structure present in inorganic and organic compounds.

PACS numbers:

## I. INTRODUCTION

The magnetism of organic<sup>1,2,3</sup> and organometallic<sup>4</sup> polymers has been a challenging topical field since its first experimental announcements. This rapidly growing and interdisciplinary research area also includes inorganic compounds<sup>5</sup>, with ferro- and ferrimagnetic long-range order (see Sec. II below). In this work we briefly review some attempts to describe the ground state and the low-temperature thermodynamics of these compounds. In particular, we report on analytical and numerical results on polymeric chains of correlated electrons in special unit cell topologies shown in Fig. 1.

## II. QUASI-ONE-DIMENSIONAL MAGNETIC COMPOUNDS: A BRIEF REVIEW

Despite many years of experimental and theoretical efforts, the complete understanding and precise characterization of magnetism and electronic correlations in quasi-one-dimensional (quasi-1d) compounds still offer great scientific challenges and technical difficulties<sup>3</sup>. Regarding, for instance, organic magnetic polymers, it is known<sup>3</sup> that their magnetic properties are ascribed to the correlated  $p$ -electrons of light elements, such as C, O, and N, in contrast to the magnetism found in transition and rare-earth metals due to partially filled  $d$  or  $f$  orbitals. For this reason it took many years of efforts on the synthesis and characterization of a great variety of compounds before the announcement of bulk ferromagnetism (FM) in an organic polymer<sup>1</sup>. In Fig. 1(b) we sketch this material made of polyacetylene-based radicals,  $R^\bullet$ , containing unpaired residual electrons, i.e., poly-BIPO or poly[1,4-bis(2,2,6,6-tetramethyl-4-piperidyl-1-oxyl)-butadiyne]. However, this compound presented several problems due to its insolubility and poor repro-

ducibility both in the preparation and in the magnetic results<sup>3</sup>. Later, Nishide and collaborators<sup>6</sup> have successfully synthesized polyphenylacetylenes with various types of radical groups. These polymers exhibit similar band structure schemes<sup>7</sup> comprising filled bonding molecular-orbital bands, empty antibonding bands, and narrow half-filled nonbonding bands, usually just one at the center of the band. A net magnetic moment may appear either because the number of itinerant antiferromagnetically (AF)-correlated electrons per unit cell is odd and/or due to the presence of localized electrons<sup>1,7</sup>.

A seminal work has also been performed by Takahashi and collaborators in order to extensively characterize the long-range macroscopic FM behavior found in the organic compound  $p$ -nitrophenyl nitroxyl nitroxide radical (p-NPNN, in the  $\alpha$  and  $\beta$  phases)<sup>2,8</sup>. Actually, the excellent fitting of the low-temperature ( $T$ ) experimental data is consistent with predictions from the thermodynamic Bethe-ansatz solution of the 1d-quantum FM Heisenberg model<sup>8</sup>: susceptibility  $\propto T^{-2}$  and specific heat  $C \propto T^{1/2}$ , as  $T \rightarrow 0$ .

Other organic magnets have been synthesized, such as polyradicals derived from poly(1,3-phenylene ethylene) and polyphenylenevinylene-based radicals<sup>3</sup>. In these cases the polymer structure is made of benzene rings linked by divalent carbon atoms or including pendant radicals with oxygen atoms carrying an uncompensated electron<sup>3</sup>. Another family of organic magnetic polymers is that of the doped poly( $m$ -aniline) compounds, in which the carbon atoms responsible for the links between the benzene rings are substituted by ionized nitrogen with a H-bond or a radical plus a charge acceptor<sup>9</sup>. On the other hand, doped polypyrrole compounds also exhibit<sup>10</sup> interesting magnetic properties and Dirude metallic response as well.

A distinct class of magnetic polymers combines metal ions with organic complexes, displaying a rich

variety of magnetic behaviors, such as ferro- and ferrimagnetism, AF and canted AF and spin glass phase<sup>11,12</sup>. In fact, the first experimental observation of a magnet with spin residing in a p-orbital was performed in the compound  $[\text{Fe}(\text{C}_5\text{Me}_5)_2]^+$  [TCNE] (TCNE = tetracyanoethylene)<sup>4</sup>. Some homometallic ferrimagnets with chain structure<sup>13,14</sup> involve the compounds<sup>15,16</sup>  $\text{M}_2(\text{EDTA})(\text{H}_2\text{O})_4 \cdot 2\text{H}_2\text{O}$  ( $\text{M} = \text{Ni}, \text{Co}$ ; EDTA = ethylenediaminetetraacetate =  $\text{C}_{10}\text{H}_{16}\text{N}_4\text{O}_8$ ) and  $\text{M}(\text{R-py})_2(\text{N}_3)_2$  ( $\text{M} = \text{Cu}, \text{Mn}$ ; R-py = pyridinic ligand =  $\text{C}_5\text{H}_4\text{N-R}$  with  $\text{R} = \text{Cl}, \text{CH}_3$ , etc.)<sup>17,18,19,20</sup>. Regarding bimetallic chain materials, the compound<sup>21</sup>  $\text{MnCu}(\text{pbaOH})(\text{H}_2\text{O})_3$  [pbaOH = 2-hydroxy-1,3-propylenebis(oxamato) =  $\text{C}_7\text{H}_6\text{N}_2\text{O}_7$ ] has been one of the first synthesized which retains long-range FM or ferrimagnetic order on the scale of the crystal lattice, as in the case of isomorphous realizations<sup>22,23,24</sup>. Heterometallic chain structures have also been object of systematic study<sup>25,26</sup>. More recently, the metal-radical hybrid strategy, combined with fabrication of novel polyradicals<sup>27</sup>, has led to the synthesis of a variety of heterospin chain compounds<sup>28,29</sup>. Several of these compounds display 1d ferrimagnetic behavior<sup>30,31</sup> modeled by alternating spin chains<sup>32</sup>, such as, for instance, those with the structure shown in Fig. 1(c).

Of recently growing interest we mention the quasi-1d chains with  $\text{AB}_2$  and  $\text{ABB}^0$  unit cell structure [henceforth referred to as  $\text{AB}_2$  chains; see Figs. 1(a) and (b)]. Such structures are found both in inorganic and organic ferrimagnetic compounds. Regarding inorganic materials, we cite the homometallic compounds with a line of trimer clusters characteristic of phosphates of formula  $\text{A}_3\text{Cu}_3(\text{PO}_4)_4$ , where  $\text{A} = \text{Ca}$ ,<sup>33,34,35,36</sup>,  $\text{Sr}$ ,<sup>34,35,36,37</sup>, and  $\text{Pb}$ <sup>35,36,38</sup>. The trimers have three  $\text{Cu}^{+2}$  paramagnetic ions of spin  $S = 1/2$  AF coupled. Although the superexchange interaction is much weaker than the intratrimer coupling, it proves sufficient to turn them into bulk ferrimagnets. Furthermore, compounds of formula  $\text{Ca}_{3-x}\text{Sr}_x\text{Cu}_3(\text{PO}_4)_4$ ,  $0 < x < 3$ <sup>37</sup>, hybrid analogous to the mentioned phosphates, have also been synthesized in an attempt to tune the AF bridges between Cu sites and possibly explore how paramagnetic spins grow into bulk ferrimagnets. It is also interesting to mention the frustrated  $\text{AB}_2$  inorganic compound<sup>39</sup>  $\text{Cu}_3(\text{CO}_3)_2(\text{OH})_2$ , which displays low-T short-range magnetic order and has its physical properties well described through the distorted diamond chain model<sup>40</sup>. At last, we observe that the  $\text{AB}_2$  structure is also present<sup>41</sup> in the organic ferrimagnetic compound 2-[3',5'-bis(N-tert-butylaminoxyl)phenyl]-4,4,5,5-tetramethyl-4,5-dihydro-1H-imidazo[1,1-oxy] 3-oxide, or PNNBNO, consisting of three  $S = 1/2$  paramagnetic radicals in its unit cell.

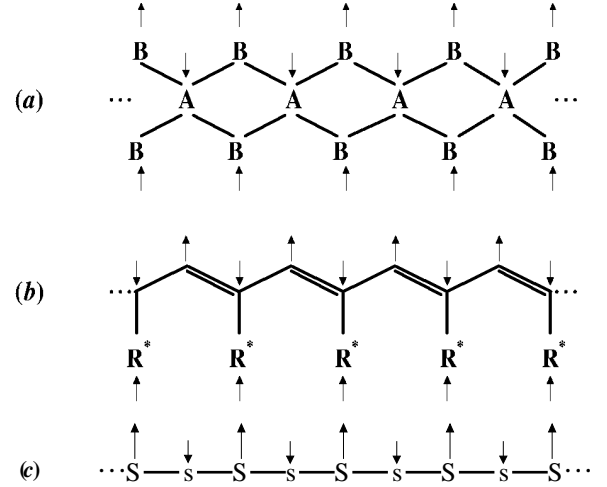


FIG. 1: Ferrimagnetic ground-state configurations of (a) bipartite lozenge  $\text{AB}_2$  chains, (b) substituted polyacetylene, with lateral radicals  $\text{R}^*$  as  $\text{B}$  sites containing unpaired residual electrons, and (c) alternate spin chains.

### III. MAGNETIC CHAINS WITH $\text{AB}_2$ UNIT CELL TOPOLOGY: ANALYTICAL AND NUMERICAL STUDIES

In this section we model and discuss analytical and numerical results on the magnetic chains with  $\text{AB}_2$  and  $\text{ABB}^0$  unit cell topologies displayed in Figs. 1(a) and (b). Eventually, alternate spin chains shown in Fig. 1(c) are also considered.

A rigorous theorem by Lieb<sup>42</sup> predicts that bipartite  $\text{AB}_2$  chains modeled through a Hubbard Hamiltonian [see Eq. (1) below], with one electron per site on average (half-filled limit) and repulsive Coulombian interaction, present average ground-state spin per unit cell  $\sim 2$  and quantum ferrimagnetic long-range order at  $T = 0$ <sup>42,43,44,45</sup>. The magnetic excitations on this state have been studied in detail both in the weak- and strong-coupling limits<sup>46</sup>, and in the light of the quantum  $\text{AB}_2$  Heisenberg model<sup>46,47,48</sup>. Further studies have considered the anisotropic<sup>49</sup> and isotropic<sup>50</sup> critical behavior of the quantum  $\text{AB}_2$  Heisenberg model, including its spherical version<sup>51</sup>, and the statistical mechanics of the classical  $\text{AB}_2$  Heisenberg model<sup>47</sup>.

Away from half-filling, doped  $\text{AB}_2$  Hubbard chains were previously studied through Hartree-Fock, exact diagonalization and quantum Monte Carlo techniques both in the weak- and strong-coupling limits<sup>43,52</sup>, including also the  $t-J$  model<sup>53</sup> using the density-matrix renormalization group and recurrent variational Ansatzes, and the infinite Coulombian repulsion limit<sup>54</sup> using exact diagonalization. In particular, these chains represent an alternative route to reaching 2d quantum physics from 1d system  $S^{53,55}$ .

## A. Analytical Results

We start considering the  $AB_2$  chain modelled through the one-band Hubbard model, which is the simplest lattice model for strongly correlated materials:

$$H = \sum_{\langle i,j \rangle} t_{ij} c_{i\sigma}^\dagger c_{j\sigma} + U \sum_i n_{i\uparrow} n_{i\downarrow}; \quad (1)$$

where  $c_{i\sigma}^\dagger$ ,  $(c_{i\sigma})$  is the creation (annihilation) operator for electrons with spin  $(\sigma = \uparrow, \downarrow)$  at site  $i = A, B_1$  or  $B_2$  of the unit cell  $i$ ,  $t$  is the hopping parameter,  $U$  is the intrasite Coulomb repulsion and, in the first summation,  $i$  and  $j$  are nearest neighbor sites. We denote  $N$  as the total number of sites and  $N_c (= N/3)$  as the number of unit cells. We remark that in the limit  $U \rightarrow \infty$ , the Hubbard Hamiltonian reduces to a hopping term with double site occupancy excluded.

In the tight-binding description ( $U \rightarrow \infty$ ), this model presents three bands: one flat with  $N_c$  localized orbitals with energy  $\epsilon = 0$  and two dispersive with  $\epsilon = \pm 2t \cos(q/2)$ , where  $q = 2\pi l/N_c$  and  $l = 0, \dots, N_c - 1$ . At half-filling ( $N_e = N$ , where  $N_e$  is the number of electrons) and  $U \rightarrow \infty$  the ground state (GS) total spin quantum number  $S_g$  is degenerate, with  $S_g$  ranging from the minimum value (0 or 1/2) to  $S_g = N_B - N_A/2 = N_c/2$ , where  $N_A$  ( $N_B$ ) is the number of sites in the A (B) sublattice. As proved by Lieb<sup>42</sup>, in the general case of any bipartite lattice with  $N_B \leq N_A$ , the Coulomb repulsion lifts this huge degeneracy and selects the state with  $S_g = N_B - N_A/2$  to be the unique GS of the system, apart from the trivial  $(2S_g + 1)$ -fold rotational degeneracy.

In the strong coupling limit ( $U \gg t$ ) and at half-filling the  $AB_2$  Hubbard Hamiltonian, Eq. (1), is mapped<sup>50,56</sup> onto the quantum  $S = 1/2$  Heisenberg model with  $O(n)$ ,  $n = 3$ , rotational symmetry:

$$H = \sum_{\langle ij \rangle} J_{ij} \mathbf{S}_i \cdot \mathbf{S}_j; \quad (2)$$

where the localized spins  $\mathbf{S}_i$  interact antiferromagnetically through  $J_{ij} = J = 4t^2/U > 0$ . In fact, Lieb and Mattis have shown<sup>57</sup> that the Heisenberg model in a bipartite lattice has also  $S_g = N_B - N_A/2$ , which indicates that  $S_g = N_c/2$  for the  $AB_2$  Heisenberg model, as in the Hubbard case. Eventually, in the presence of an uniform magnetic field  $H$  along the  $z$  direction a Zeeman energy term,  $\mathcal{H}_B = \sum_i g_B \mu_B S_i^z$ , is added to Eq. (2), where  $g$  is the gyromagnetic factor and  $\mu_B$  is the Bohr magneton (in what follows we take units in which  $g_B = 1$ ). In  $H = 0$  the ground-state of the system exhibits<sup>42,43</sup> unsaturated FM or ferrimagnetic correlations as indicated in Figs. 1 (a) and (b), with average spin per unit cell  $\langle S_{\text{cell}}^z \rangle = \sim 2$  (Lieb's theorem<sup>42</sup>). In addition, we can also model the alternate spin chains shown in Fig. 1 (c) by considering in Eq. (2)  $S_i = S_1$  and  $S_i = S_2$ , with  $S > s$ . Such model systems have been used to

describe<sup>31,32</sup> a number of organometallic compounds in which, e.g.,  $S = 5/2$  or  $S = 2$  and  $s = 1/2$ .

The Euclidean action of the partition function in a coherent-state  $n$ -eld representation<sup>58</sup>,  $Z = \int Dn \exp(-S_E)$ , is given by  $S_E = S_{\text{exc}} + S_{WZ} + S_Z$ , with contributions from exchange and Zeeman interactions, and a topological Wess-Zumino term, which is a Berry's phase-like term associated with the time evolution of the spin due to quantum fluctuations<sup>58</sup>. The low-lying properties of the quantum ferrimagnetic chains in Fig. 1 are dominated by infrared fluctuations around the Neel configuration. In order to obtain their effective low-lying action, we take staggered dimensionless unit coherent magnetization elds and split the topological term in a FM and an AF contribution,  $S_{WZ} = S_{WZ}^{\text{AF}} + S_{WZ}^{\text{FM}}$ , following the spin structure of the polymer. Then, taking the continuum limit and integrating out the rapidly fluctuating eld modes, we obtain the low-energy effective action,  $S_{\text{eff}} = \int_0^L dx (2a) \int_0^{\sim} dL$ , where  $L$  is the length of the chain of lattice parameter  $2a$ , and  $(\hbar T)^{-1} = it \sim$  expresses the result of a Wick rotation to imaginary times  $it$ . The Lagrangian density is  $L = L_{NL} + L_{WZ}^{\text{FM}} + L_Z + L_{\text{irrel}}$ , where

$$L_{NL} = L_{\text{exc}} + L_{WZ}^{\text{AF}} = \frac{1}{2} (\partial_x m)^2 + \frac{1}{2} (\partial_m m)^2; \quad (3)$$

corresponds to the quantum nonlinear (NL) model, with unit magnetization elds  $m^2 = 1$ ,

$$L_{WZ}^{\text{FM}} = \frac{1}{2} \int_0^L dx \int_0^{\sim} dL (\partial_m m)^2; \quad (4)$$

represents the contribution from the FM Wess-Zumino term, and  $L_{\text{irrel}}$  are irrelevant terms in the renormalization group (RG) context. In Eqs. (3) and (4),  $\partial_x = 2JS^2/a^2$ ,  $\partial_m = 1/(8J)$ , and  $S = S$  for the  $AB_2$  chains, whereas  $\partial_x = JS^2/a^2$ ,  $\partial_m = s/(4JS)$ , and  $S = S$  for the alternate spin chains of Fig. 1. The FM Wess-Zumino term is responsible for the ferrimagnetic ground states. Indeed,  $L_{WZ}^{\text{FM}} = 0$  in either cases of AB or S = s chains. Those represent usual quantum AF Heisenberg chains, which are known to follow Haldane's conjecture<sup>59</sup>, i.e., half-integer spin chains are critical with no long-range order, and integer spin chains are disordered. Moreover, the addition of the relevant Wess-Zumino term to the quantum NL model, Eq. (3), changes its properties dramatically since the critical dynamical exponent assumes  $z = 2$  (nonrelativistic feature), in contrast with the value  $z = 1$  found in the relativistic quantum NL model, associated with the 2d-quantum AF Heisenberg Hamiltonian. In fact, Eq. (4) corresponds to the eld-theoretical version of the topological constraints imposed by the polymer structure, as identified by semi-empirical methods<sup>1,60,61</sup>.

We now perform a momentum-shell low- $T$  RG study of the system (see<sup>62</sup> and<sup>63</sup> to similar treatments to the classical and quantum  $z = 1$  NL models). First, we decompose the magnetization elds into transversal and longitudinal components, integrate over the latter one, expand

the resulting action,  $S_{\text{eff}} = S^{(2)} + S^{(4)} + \dots$ , and Fourier transform the terms to the momentum  $\mathbf{k}$  and Matsubara frequency- $\omega_n$  space, with  $\omega_n = 2\pi n u$ ,  $n = 0; \pm 1; \pm 2; \dots$ ,

$u = \frac{1}{m}$ , and  $\omega_n = 2JS\omega^2$  or  $\omega_n = 2JSs\omega^2 = (S/s)\omega$  respectively for the  $AB_2$  or alternate spin chains. The quadratic term in the diagonal field space  $\phi; g$  reads<sup>50</sup>

$$\frac{S^{(2)}(\mathbf{k}; \omega_n)}{\sim} = \sum_{n=1}^{\infty} \int_{BZ} \frac{d^d k}{(2\pi)^d} \frac{u}{g_0} (\mathbf{k}^2 - i\omega_n + hg_0 + \frac{d}{2} \omega_n^2 - \frac{g_0}{u})^{-1} (\mathbf{k}; \omega_n) (\mathbf{k}; \omega_n); \quad (5)$$

where  $hg_0 = H/\omega_n$ , the density of degrees of freedom comes from the integration over the longitudinal components, and the meaning of  $d$  is discussed below. The

bare coupling is defined as  $g_0 = S$  in  $d = 1$ . The quartic contribution is given by<sup>50</sup>

$$\begin{aligned} \frac{S^{(4)}(\mathbf{k}_i; \omega_{n_i})}{\sim} = & \sum_{n_1, \dots, n_4=1}^{\infty} \int_{BZ} \frac{d^d k_i}{(2\pi)^d} \frac{u}{g_0} \\ & \left[ \frac{1}{2} (\mathbf{k}_2 - \mathbf{k} + \mathbf{k}_2 - \mathbf{k} + \mathbf{k}_1 - \mathbf{k} - \mathbf{k}_1 - \mathbf{k}) + \frac{i hg_0}{2^{1=2}} \sum_{j=1}^d (\mathbf{k}_{j4} - \mathbf{k}_{j3}) \right. \\ & + \frac{hg_0}{2} \left[ \frac{i}{4} (\omega_{n_3} + \omega_{n_4}) - \frac{1}{2^{1=2}} \sum_{j=1}^d (\omega_{n_3} k_{j4} - \omega_{n_4} k_{j3}) \right. \\ & + \left. \frac{11}{96} \frac{1}{2} (\omega_{n_1} \omega_{n_3} + \omega_{n_1} \omega_{n_4} + \omega_{n_2} \omega_{n_3} + \omega_{n_2} \omega_{n_4}) \right] \\ & \left. (\omega_{n_1} - \omega_{n_2} - \omega_{n_3} - \omega_{n_4}) \right] \frac{1}{(2\pi)^d} (\mathbf{k}_2 + \mathbf{k}_4 - \mathbf{k}_1 - \mathbf{k}_3) (\omega_{n_2} + \omega_{n_4}) (\omega_{n_1} + \omega_{n_3}); \end{aligned} \quad (6)$$

In the sequence, we require that the fluctuation modes in the two-point vertex function scales homogeneously through a RG scaling transformation,  $\mathbf{k} \rightarrow b\mathbf{k}$ ,  $\omega_n \rightarrow b^z \omega_n$ , with  $b \rightarrow e^\ell$ . We also take the fixed point  $d = 0$  for  $d = 1$ , as a consequence of the irrelevance of the  $\omega_n^2$ -dependent terms in the RG context. The one-loop equations for the renormalized coupling  $g$ , and dimensionless temperature  $t = g/u$  and magnetic field  $h = hg_0$  in  $d = 1$  and  $z = 2$  read<sup>50</sup>:

$$\begin{aligned} \frac{dg}{d\ell} &= (d+z-2)g + \frac{d}{2} g^2 \coth[g(1+h)=2t]; \\ \frac{dt}{d\ell} &= (d-2)t + \frac{d}{2} g t \coth[g(1+h)=2t]; \\ \frac{dh}{d\ell} &= 2h; \quad \frac{du}{d\ell} = -zu; \quad u = \frac{g}{t}; \end{aligned} \quad (7)$$

We thus obtain the semiclassical fixed point:  $g = t = h = 0$ , since  $g = 0$  implies in  $S \rightarrow 1$ , and the quantum critical fixed point<sup>63</sup>:  $g = g_c = 2$ ;  $t = h = 0$ . The former describes a 1d-classical Heisenberg ferromagnet with quantum corrections, whereas the latter is identified with a classical Heisenberg model in  $d+z = 3$  dimensions. The analysis of stability shows that both

fixed points are unstable under thermal fluctuations, but only the semiclassical fixed point is stable under infrared quantum fluctuations, as shown in Fig. 2.

By studying the correlation length and magnetic susceptibility we identify<sup>50</sup> three distinct quantum regimes. As  $T \rightarrow 0$  and  $g > g_c$ , the quantum  $z = 2$  NL model is in a quantum disordered phase, whereas for  $g < g_c$  its ground state has long-range order, with both quantum and thermal fluctuations playing important roles. For  $g = g_c$  and  $T \rightarrow 0$  the system approaches the quantum critical fixed point characterized by the extinction of the spin-wave modes and the absence of long-range order. As shown in Fig. 2, the quantum critical region is defined by the crossover lines  $T \propto g^j$ , where  $j = z/3$ , with  $3$  the 3d-Heisenberg correlation-length exponent. In particular, we find<sup>50</sup> the following low- $T$  behavior in the quantum critical region:

$$T^{1=z}; \quad T^{-1}; \quad C \propto T^{d=z}; \quad (8)$$

with the standard result for the low- $T$  quantum critical specific heat  $C$  and exponents satisfying scaling relations proper of this region<sup>64,65</sup>. Similarly, for the  $T \rightarrow 0$ ,  $g <$

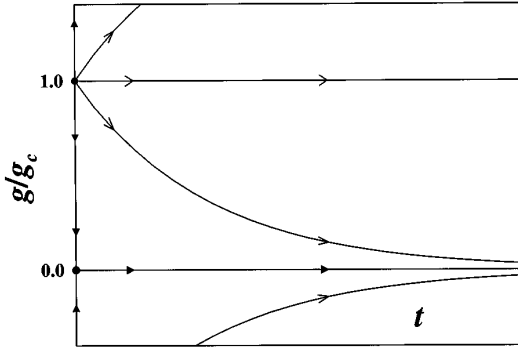


FIG. 2: Schematic RG ( $g;t / T$ ) ux diagram for the 1d-quantum  $z = 2$  NL model. Semiclassical ( $g = T = 0$ ) and quantum-critical ( $g = g_c; T = 0$ ) fixed points are shown, as well as the ux lines indicating their stability with respect to infrared perturbations. The segment  $T = 0; 0 < g_0 < g_c$ , corresponds to the loci of points in which Lieb's theorem is included, with presence of stable ferrimagnetic states of quantum  $AB_2$  and alternate spin chains.

$g_c$  semiclassical region, we find

$$T^{-1}; \quad T^{-2}; \quad C \quad T^{-1/2}; \quad (9)$$

where the specific heat is determined by the spin wave contribution. In Eqs. (8) and (9) the amplitudes of the observables cannot be completely fixed by the RG procedure. We thus identify the asymptotic low- $T$  critical behavior described by Eq. (9) with that of the quantum  $S = 1/2$   $AB_2$  and alternate spin ferrimagnetic chains, as well as that of the 1d-quantum  $S = 1/2$  Heisenberg ferromagnet, such as the organic ferromagnetic compound p-NPNN<sup>8</sup>. In addition, an interesting question arises regarding the access of such  $AB_2$  chains in the half-filled strong-coupling limit to the quantum disordered and quantum critical regimes of the quantum  $z = 2$  NL model. This scenario, if accomplished, might involve the presence of extra frustrated couplings in the unit cell structure. In any case, we would like to mention that our predicted one-loop critical behaviors for the renormalized classical and quantum critical fixed points are in agreement with those of the FM transition in 1d itinerant electron systems in the context of a Luttinger liquid framework<sup>66</sup>. However, while our localized spin disordered phase is gapped, the quantum disordered phase in Ref.<sup>66</sup> behaves as an ordinary gapless Luttinger liquid. Obviously, further theoretical work is needed in order to clarify the physical scenario predicted for the critical behavior of the quantum NL model with a FM Wess-Zumino term due to the  $AB_2$  topology.

In order to improve the understanding of the role of the quantum and thermal fluctuations, topology, and spin symmetry to the properties of the ferrimagnetic  $AB_2$  chains, we have also performed a number of analytical studies using Ising, Heisenberg and spherical Hamiltonians as model systems in this unit cell structure<sup>47,51,67</sup>.

First, by regarding the spin operators in Eq. (2) as Ising variables,  $S_i = \pm 1/2$ , we apply<sup>47</sup> the RG decimation of B sites and obtain the exact Gibbs free energy as function of the effective coupling  $J$  and field  $H$ . At zero field the ground state result  $J = -2J < 0$  for the effective coupling between A sites indicates the presence of a ferrimagnetic structure with average spins at B sites pointing opposite to those at A sites, implying in a unit cell average spin  $\langle S_{\text{cell}}^z \rangle = -1/2$ . As  $H$  increases at  $T = 0$ , we notice that  $J$  increases linearly with  $H$  and vanishes for  $H = J$ ; conversely,  $H$  first decreases linearly with  $H$  for  $H < J$ , and then increases also linearly, changing sign at the critical field  $H_c = 2J$ . At  $H = H_c$  a first order transition occurs with a discontinuous change of  $\langle S_{\text{cell}}^z \rangle$  from  $-1/2$  to its saturated value  $3/2$  (see Fig. 3). At finite temperatures the described effects are less dramatic, and the unit cell average spin grows continuously with the field from 0 at  $H = 0$  (disordered state at finite  $T$ ) to the saturated value  $3/2$  as  $H \rightarrow \infty$ . The  $H = 0$  results are corroborated by the calculation of the two-spin correlation function, which is related to the susceptibility through the fluctuation-dissipation theorem. Actually, we have also found that  $\exp[J/(k_B T)] = (k_B T)$ ,

leading to the relation between the corresponding critical exponents  $\nu = 2$ , and from the behavior of the correlation function at  $T = 0$  and magnetization at  $T = 0$  and  $H \rightarrow 0$  it follows that  $\beta = 1$  and  $\gamma = 1$ . This set of exponents belongs to the same class of universality of decorated 1d ferromagnetic Ising system<sup>68</sup>.

Now, by considering Heisenberg spins in a classical context, in which quantum fluctuations are absent, the low- $T$  and high- $T$  limits of the  $H = 0$  free energy and two-spin correlation functions have been calculated<sup>47</sup>. It is instructive to compare the  $T \rightarrow 0$  result obtained for the

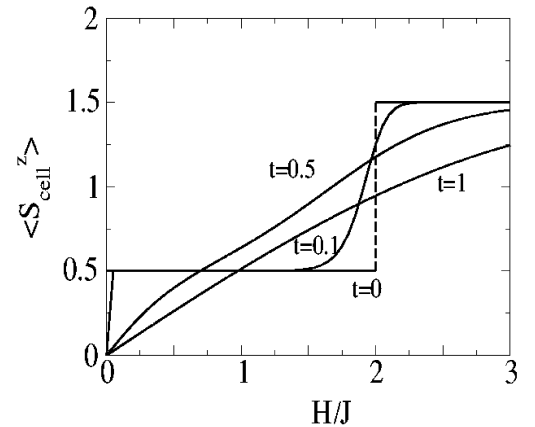


FIG. 3: Average spin per unit cell,  $\langle S_{\text{cell}}^z \rangle$ , in units of  $1/2$ , as function of the dimensionless magnetic field,  $H/J$ , and dimensionless temperature,  $t = k_B T/J$ , for the ferrimagnetic  $S = 1/2$   $AB_2$  Ising chain.

classical ferrimagnetic  $AB_2$  Heisenberg chain,

$$= \frac{2}{9} \frac{J}{(k_B T)^2} \left[ 1 - \frac{13}{4} \frac{k_B T}{J} + \dots \right]; \quad (10)$$

with that of the classical ferrimagnetic linear Heisenberg chain<sup>69</sup>,

$$= \frac{2}{3} \frac{J}{(k_B T)^2} \left[ 1 - \frac{1}{2} \frac{k_B T}{J} + \dots \right]; \quad (11)$$

and that of Takahashi<sup>8</sup> for the quantum ferrimagnetic spin-1/2 linear Heisenberg chain,

$$= \frac{2}{3} \frac{J}{(k_B T)^2} \left[ 1 - \frac{3}{(2)^{1=2}} \frac{(k_B T)^{1=2}}{J^{1=2}} + \frac{3}{2} \frac{(1=2) k_B T}{J} + \dots \right]; \quad (12)$$

where  $(1=2) = (2)^{1=2} = 0.583$ . At low- $T$  Fisher's and Takahashi's leading terms coincide and are three times larger than that of the  $AB_2$  chain, due to the unit-cell topology effect. Moreover, the second term in Eq. (12), absent in the classical models, is related to the mixing of the anomalous entropy and specific heat classical behaviors when quantum fluctuations are not present. We notice that this  $T^{-2}$  leading result as  $T \rightarrow 0$  has also been obtained for the semiclassical fixed point of the quantum  $z = 2$  NL model, related to the quantum  $AB_2$  Heisenberg chains (see above).

By taking quantum fluctuations into account, we also calculate<sup>67</sup> the three spin-wave modes of the quantum spin-1/2  $AB_2$  Heisenberg model using the Holstein-Primakoff transformation and subsequent diagonalization via the Bogoliubov-Tyablikov method, namely, one non-dispersive optical,  $\omega_k^a$ , one dispersive optical,  $\omega_k^b$ , and one acoustical mode,  $\omega_k^c$ :

$$\begin{aligned} \omega_k^a &= J + H; \\ \omega_k^{b,c} &= \frac{J}{2} \sqrt{1 + [1 + 8 \sin^2(ka)]^{1=2}} g \pm H; \end{aligned} \quad (13)$$

notice in the acoustical mode the presence of a quadratic ferrimagnetic dispersion relation  $\omega_k^c = 2J(ka)^2$ ,  $ka \ll 1$ ,  $H = 0$ . From this result, corrections due to quantum fluctuations to the average values  $\langle S_B^z \rangle = \langle S_A^z \rangle = \sim 2$  are derived, although the result of Lieb's theorem,  $\langle S_{\text{cell}}^z \rangle = \sim 2$ , remains true. In a mean-field approach<sup>47,67</sup>, we relate the quantum thermal spin averages at sites A and B to the respective Weiss molecular fields and find, in the simplest case in which they are assumed to be parallel to the  $z$  direction (Ising-like solution):  $\langle S_B^z \rangle = \sim 2$  for all  $H \geq 0$ , and  $\langle S_A^z \rangle = \sim 2$  for  $0 \leq H < H_c$ , whereas  $\langle S_A^z \rangle = \sim 2$  for  $H > H_c$ . We notice that  $H_c = 2J$  is the critical field below which the ferrimagnetic ordering is favoured, in agreement with the above result for the spin-1/2  $AB_2$  Ising model. Indeed, the unit cell spin reads  $\langle S_{\text{cell}}^z \rangle = \sim 2$  for  $0 < H < H_c$ , and  $\langle S_{\text{cell}}^z \rangle = 3 \sim 2$  for  $H > H_c$ . On the other hand, in the case the  $x$  and  $y$  components are also considered, a quite interesting scenario emerges, with

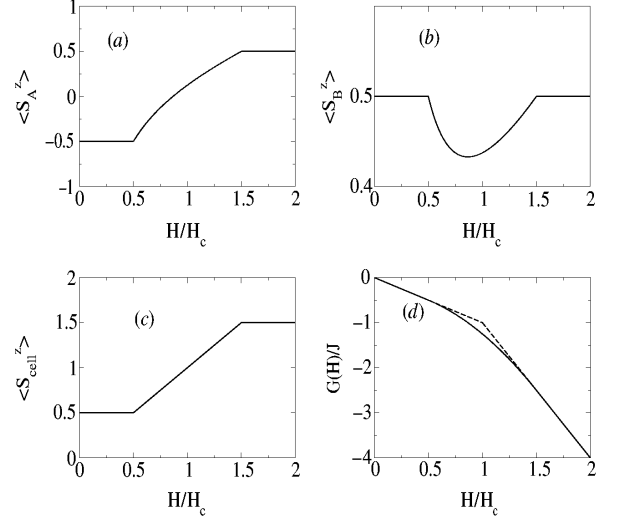


FIG. 4: Average spin at sites A (a), sites B (b) and per unit cell (c), in units of  $\sim$ , as function of the reduced field,  $H = H_c$ , for the quantum ferrimagnetic  $S = 1=2$   $AB_2$  Heisenberg chain, with  $H_c = 2J$ . (d) The field dependence of the Gibbs free energy shows that the continuous solution (solid line) for the magnetization is the stable phase. The Ising-like solution is shown for comparison (dashed line).

$\langle S^z \rangle = \sim 2$  for  $0 \leq H < H_c = 2$ , and  $\langle S^z \rangle = \sim 2$  for  $H > 3H_c = 2$ , where the plus (minus) sign refers to  $\langle S_B^z \rangle$  ( $\langle S_A^z \rangle$ ) sites; for intermediate fields,  $H_c = 2 < H < 3H_c = 2$ , one has that  $\langle S_A^z \rangle = \sim [3H_c - (4H - H_c)]/2$  and  $\langle S_B^z \rangle = \sim [3H_c - (8H - H_c)]/2$ . These results imply in the unit cell average spin  $\langle S_{\text{cell}}^z \rangle = \sim 2$  for  $H < H_c = 2$ , with ferrimagnetism sustained, and the saturated  $3 \sim 2$  value for  $H > 3H_c = 2$ , as in the Ising-like solution. A linear increase with  $H$  arises for intermediate fields:  $\langle S_{\text{cell}}^z \rangle = H/H_c$ , for  $H_c = 2 < H < 3H_c = 2$  (see Fig. 4). In this regime the average spin at sites A continuously rotates seeking a full alignment with  $H$ , accompanied by a rotation of the spins at sites B, such that the transversal spin components at sites A and B always cancel out. To achieve this cancellation the spins at sites B rotate in the opposite direction up to a maximum polar angle  $\theta = \pi/6$  and then rotate back [see Fig. 4 (b)]. These results are corroborated by the analysis of the Gibbs free energy [Fig. 4 (d)].

At last, a spherical version of the quantum  $AB_2$  spin Hamiltonian has also been studied<sup>51</sup>. For this purpose, a chemical potential ( $\mu$ ) term is added to Eq. (2) in order to take care of the spherical constraint,  $\sum_i \langle S_i^2 \rangle = N/4$ , where  $N$  is the total number of sites. Quantum fluctuations are introduced, associated with a quantum coupling parameter  $g$ , through a kinetic energy term  $(g/2) \sum_i P_i^2$ , in which  $P_i$  are momentum operators canonically conjugated to each spin degree of freedom. By diagonalizing the Hamiltonian in a space of proper bosonic operators, we obtain two dispersive eigenmodes, also present in the linear AF spherical model, and a flat

band induced by the  $AB_2$  topology. At the only critical point,  $g = T = H = 0$ , the ferrimagnetic long-range order is present with  $\langle S_B^z \rangle = \langle S_A^z \rangle = \sim 3/4$  and  $\langle S_{\text{cell}}^z \rangle = \sim (2/3) = 8/12$ . Interestingly, in the quantum  $AB_2$  spherical case the average spin per unit cell is less than  $\sim 2$ , in contrast with the result of Lieb's theorem for the  $AB_2$  Hubbard model in the strong-coupling half-

filled limit and the quantum  $AB_2$  Heisenberg chain with AF couplings. Calculation of the correlation functions at  $g = T = H = 0$  show that they are distance independent and finite, consistently with the ferrimagnetic order and the spherical constraint. Outside this critical point, for any finite  $g$ ,  $T$  or  $H$ , quantum and/or thermal fluctuations destroy the long-range order in the system, which in this case displays a finite maximum in the susceptibility. In this regime spins remain ferrimagnetically short-range ordered to some extent in the  $fg;T;H$  parameter space as a consequence of the AF interaction and the  $AB_2$  topology. Indeed, we notice in Fig. 5 that, although the field-induced unit cell average spin,  $\langle S_{\text{cell}}^z \rangle$ , displays quantum paramagnetic behavior for any finite  $g$  or  $T$ , the spins at sites A and B can display opposite orientations depending on the values of  $g$ ,  $T$  and  $H$ . Therefore, for special regions of the parameter space  $fg;T;H$  spins at sites A points antiparallel with respect to those at sites B, thus giving rise to a rapid increase in the unit cell average spin for very low  $H$  and a field-induced short-range ferrimagnetism, which is destroyed for large  $g$ ,  $T$  or  $H$ . In addition, to better characterize the approach to the  $g = T = H = 0$  critical point, we have considered several paths. For  $T \neq 0$  and  $g = H = 0$  the susceptibility behaves as  $T^{-2}$ , as also found in several classical and quantum spherical and Heisenberg models (see above). On the other hand, for  $H \neq 0$  and  $g = T = 0$ , we find  $H^{-1}$ , and for  $g \neq 0$  and  $T = H = 0$ ,  $\exp(cg^{-1/2})$ , where  $c$  is a constant, evidencing an essential singularity due to quantum fluctuations. In any path, the relation  $\chi \sim T^{-2}$  is satisfied. We also mention that the known drawback of classical spherical models as  $T \neq 0$  regarding the third law of thermodynamics (finite specific heat and diverging entropy) is fixed in the presence of quantum fluctuations,  $g \neq 0$ .

## B. Numerical Results

The ferrimagnetic ordering can be probed through the magnetic structure factor:

$$S(\mathbf{q}) = \frac{1}{N} \sum_{i,j} e^{i\mathbf{q} \cdot (\mathbf{x}_i - \mathbf{x}_j)} \langle S_i^z S_j^z \rangle \quad (14)$$

The condition for a long-range ferrimagnetic ordering is that  $S(0) \neq 0$ ; while  $S(\mathbf{q}) \neq 0$  in a long-range antiferromagnetically ordered state; A ferrimagnetic long-range ordering fulfill these two conditions:  $S(0) \neq 0$  and  $S(\mathbf{q}) \neq 0$ . This is the case for the  $AB_2$  Hubbard and Heisenberg chains as exemplified in Fig. 6 through

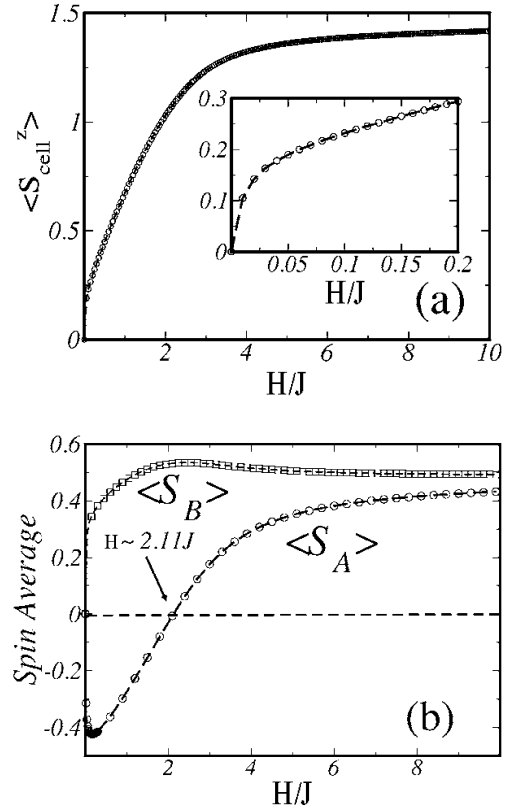


FIG. 5: (a) Average spin per unit cell,  $\langle S_{\text{cell}}^z \rangle$ , and (b) spin averages at sites A (—) and B (---), in units of  $S$ , as function of  $H/J$ , for  $g = 0.05J$  and  $T = 0.05J$ , calculated for the quantum spherical  $S = 1/2$   $AB_2$  model. Inset of (a): very-low-field regime.

the exact diagonalization (ED) of finite clusters. Due to the critical nature of both chains at low temperatures, the correlation length and  $\langle q = 0 \rangle = S(q = 0) = (k_B T)$  satisfy power law behavior:  $\chi \sim T^{-2}$  and  $\xi \sim T^{-1}$  as  $T \rightarrow 0$ . Since  $N$  at  $T = 0$ , using scaling arguments and the results of Fig. 6, we have  $T \sim T_c = T_c$ , i.e.,  $\nu = 1$ , in agreement with the values  $\nu = 2$  and  $\nu = 1$  derived using renormalization group techniques. Furthermore, the ferrimagnetism of the model was also manifested through Hartree-Fock and Quantum Monte Carlo methods<sup>43</sup>.

Systems with a ferrimagnetic GS naturally have ferromagnetic (lowering the GS spin) and antiferromagnetic (raising the GS spin) magnons as their elementary magnetic excitations. The  $AB_2$  chain have three spin wave branches<sup>46</sup>: an antiferromagnetic mode (AF mode), denoted as  $E_{S+}(q) = E(S^z = S_g + 1; q) = E_{GS}$ ; and two ferromagnetic ones (F1 and F2 modes), derived from  $E_{S-}(q) = E(S^z = S_g - 1; q) = E_{GS}$ , where  $E_{GS}$  is the GS energy and  $E(S^z; q)$  are lowest energies in the sector  $fS^z; q$ , with the lattice wave-vector  $q = 2\pi l/N_c$ , where  $l = 0; 1; \dots; N_c - 1$ . These modes are depicted in

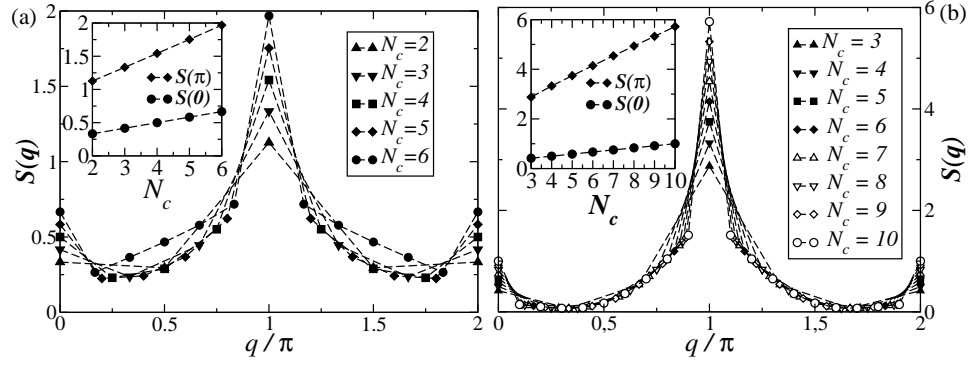


FIG. 6: Magnetic structure factor  $S(q)$  for (a) the  $AB_2$  Hubbard chain with  $U = 2t$  and (b) the  $AB_2$  Heisenberg chain. The inset presents the size dependence of the ferromagnetic [ $S(0)$ ] and antiferromagnetic [ $S(\pi)$ ] peaks. Dashed lines are guides for the eye.

Fig. 7 (a) for the Heisenberg model: the AF mode has a gap  $s_+ = 1.7591J$ ; the gapless F1 mode is the Goldstone mode, consistent with the symmetry broken phase of the chain; and the F2 mode has a gap  $s_- = 1.0004J$ . The gapped F2 branch is flat and is associated with the formation of a singlet state between the B sites in one cell, while the other cells have B sites in triplet states, as illustrated in Fig. 7 (b). The localized nature of the excitation is associated with the Hamiltonian invariance under the exchange of the B sites of any cell, this symmetry implies that the many-body wave function has a definite parity under the exchange of the spacial variables associated with these sites. Since these dispersive modes preserve the local triplet bond, they are identical to those found in the  $\text{spin-}\frac{1}{2}/\text{spin-}1$  chain<sup>70</sup>. Surprisingly, Linear Spin Wave Theory<sup>67</sup> predicts that  $s_- = 1$ , very close to our estimated value:  $s_- = 1.0004J$ . Moreover, a good agreement is found for the gapless F1 branch in the long wave-length limit. However, both LSWT and mean field theory<sup>47</sup> predicts  $s_+ = 1$ , deviating from our estimated exact diagonalization value:  $s_+ = 1.7591J$ , which is in excellent agreement with numerical and analytical calculations for the  $\text{spin-}\frac{1}{2}/\text{spin-}1$  chain<sup>70</sup>. On the other hand, the Interacting Spin Wave Theory<sup>48</sup> derives a better result for  $s_+$ , but it implies a higher shift for  $s_-$  (at mode) not observed in our data of Fig. 7 (a).

On the other hand, the AF mode is relevant in the analysis of the response to an applied magnetic field  $H$ . The AF gap found above is responsible for a plateau in the curve of the magnetization per spin [ $m(H) = \hbar S^z i = (N \sim)$ ] as a function of  $H$ . In fact, it has been shown<sup>71</sup> that if  $(s_- m) = \text{integer}$ ; a plateau may appear in the magnetization curve of the Heisenberg model. In the last equation,  $s$  is the site spin quantum number and  $m$  is the number of sites in one unit cell of the GS for a given value of  $H$ . The  $AB_2$  Heisenberg chain has  $s = 1/2$  and three sites per unit cell ( $\ell = 3$ ); so, unless the system spontaneously breaks the translation invariance, we expect plateaus at  $m = 1/6$  and  $m = 1/2$ . This is indeed what is observed in Fig. 8. The plateau width at  $m = 1/6$  is

exactly given by  $s_+$ , and is a measure of the stability of the ferromagnetic phase. For higher fields, the magnetization increases in the expected way<sup>71</sup>, as shown by the full line in Fig. 8, before saturation at  $m = 1/2$  for  $H = 3J$ . This field-dependent behavior contrasts with the linear one predicted by mean-field theory<sup>47</sup> shown in Fig. 3. Exact diagonalization results<sup>46</sup> indicate that the antiferromagnetic spin gap and, consequently, the plateau at  $m = 1/6$  exists for any finite value of  $U$ , with the plateau width ( $s_+$ ) nullifying as  $U \rightarrow 0$ .

Away from half-filling<sup>43,52</sup>, the  $AB_2$  Hubbard model exhibits a rich phase diagram depending on the electronic

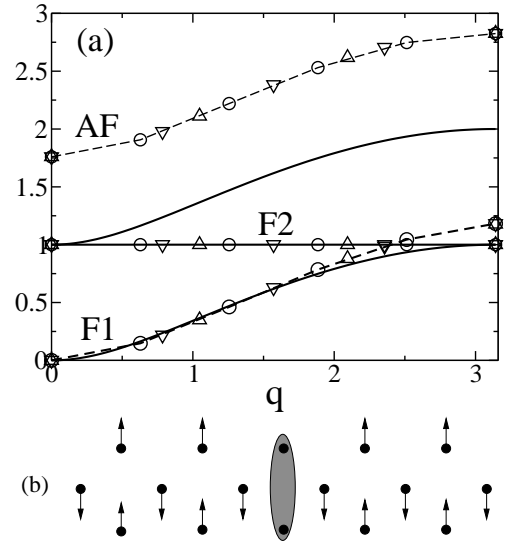


FIG. 7: (a) Ferromagnetic (F) and antiferromagnetic (AF) spin wave modes of the Heisenberg  $AB_2$  chain for  $N_c = 10$  (circles), 8 (triangles down), 6 (triangles up). Solid lines are the Linear Spin Wave results from Ref.<sup>67</sup>; dashed lines are guides to the eye. (b) Illustration of the F2 mode: ellipse indicates a localized singlet state.



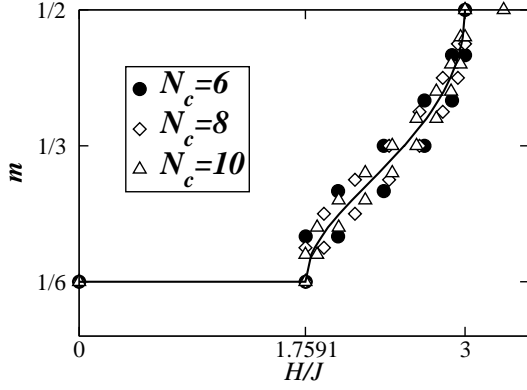


FIG. 8: Magnetization as a function of the dimensionless applied magnetic field  $H/J$  for the  $AB_2$  Heisenberg chain. The full line is a curve traced from the midpoints of the steps found in the finite size results, except at plateau regions.

density,  $n = N_e/N$ , or doping ( $= 1 - n$ ) from half-filling, and the Coulomb coupling  $U$ . The doped region was analyzed through Hartree-Fock<sup>43</sup>, exact diagonalization<sup>43,52</sup> and density matrix renormalization group (DMRG)<sup>52</sup>, which is the state-of-the-art method<sup>72</sup> for the study of the GS properties of one-dimensional quantum lattice models. DMRG results suggest that in the underdoped region and for  $U = 2t$ , the ferrimagnetic phase sustains up to  $0.02$  while for  $0.02 < \delta < 0.07$  hole itinerancy promotes incommensurate spin correlations (a spiral phase<sup>73</sup>) with a  $\delta$ -dependent peak position in the magnetic structure factor, as shown in Fig. 9 (a) and (b). For  $U = 1$  and  $\delta = 0$  the GS total spin is degenerate, whereas for  $0 < \delta < 0.225$  hole itinerancy (Nagaoka mechanism<sup>74,75</sup>) sets a fully polarized GS, as shown in Fig. 9 (c).

For higher doping, the system phase separates<sup>76</sup> into coexisting metallic and insulating phases for  $\delta_{PS}(U)$ .  $\delta < 1/3$  [with  $\delta_{PS}(1) = 0.225$  and  $\delta_{PS}(2) = 0.07$ ]. In fact, the Hartree-Fock solution is unstable in this region and a Maxwell construction is needed<sup>43</sup>. The local parity symmetry is even (odd) in the insulating (metallic) phase. In Fig. 10 we present spin correlation functions at  $\delta = 0.18$  ( $\delta = 0.28$ ) and  $U = 2$  ( $U = 1$ ) calculated through DMRG (for these parameter values, the system is found in a phase separated state). In Fig. 10(a) the correlation function between the spin at the extreme site of the phase with odd parities and the others spins,  $\langle S_1 \cdot S_L \rangle$ , evidences the spiral phase for  $U = 2t$ . For  $U = 1$  the local magnetization at sites  $A$  and  $B_1 + B_2$  shown in Fig. 10(b) clearly displays the coexistence between the Nagaoka ferrimagnetic phase and a paramagnetic one. Notice that, in the Nagaoka phase, the magnetization displays spatially modulated profiles due to hole itinerancy. Further, the local parity symmetries of the two coexisting phases are manifested in the correlation function between  $B$  spins at the same cell,  $\langle S_{B_1} \cdot S_{B_2} \rangle$ , shown in Figs. 10(c)

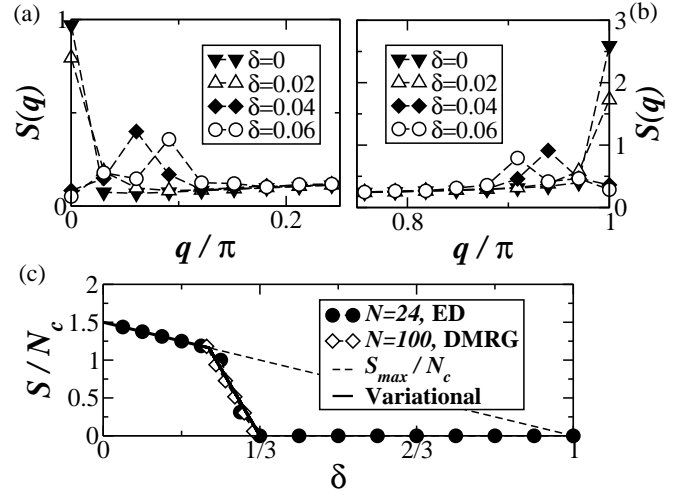


FIG. 9: (a) and (b): Magnetic structure factor for  $U = 2t$  and  $N = 100$ , using DMRG, in the underdoped region. (c) Total spin per cell  $S_g/N_c$  as function of  $\delta$  for  $U = 1$ ; the variational approach is described in Ref.<sup>52</sup>

and (d): in the phase with odd (even) parities cell triplet (singlet) states predominate. In Fig. 10(e) we illustrate the phase separation for  $U = 1$ . DMRG and exact diagonalization results<sup>52</sup> indicate that the phase separation region ends precisely at  $\delta = 1/3$ . For this doping the electronic system presents finite spin and charge gaps with very short ranged correlations and is well described by a short-ranged resonating-valence bond (RVB) state<sup>77</sup>, with the electrons correlated basically within a cell, as illustrated in Fig. 10(f). A crossover region is observed for  $1/3 < \delta < 2/3$ , while a Luttinger-liquid behavior<sup>78</sup> can be explicitly characterized for  $\delta > 2/3$ . Luttinger liquids are paramagnetic metals in one-dimension exhibiting power-law decay of the charge and spin correlation functions and the separation of the charge and spin excitation modes. In particular, the asymptotic behavior of the spin correlation function is given by

$$C_{LL}(l) \sim \frac{\cos(2k_F l) [\ln(l)]^{1/2}}{l^{1+K}}; \quad (15)$$

where  $k_F$  is the Fermi wave vector and  $K$  is the model-dependent exponent. The predicted behavior in Eq. (15) fits very well the DMRG data at  $\delta = 88/106$  using  $K = 0.89$  ( $U = 2t$ ) and  $K = 0.57$  ( $U = 1$ ), as shown in Fig. 11. We remark that these values are close to 1 (noninteracting fermions) and  $1/2$  (noninteracting spinless fermions) for  $U = 2t$  and  $U = 1$ , respectively.

In addition, we mention that the commensurate doping  $\delta = 2/3$  is insulating, with a charge gap nullifying with  $U$  in a similar manner as the one of the Hubbard model in a linear chain at half-filling<sup>79</sup>, while the spin excitation is gapless.

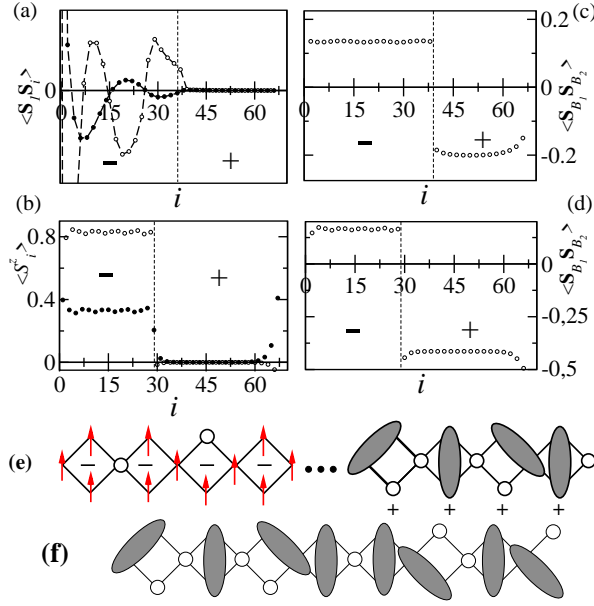


FIG. 10: GS properties at  $\beta = 0.18$  ( $U = 2t$ ) and  $\beta = 0.28$  ( $U = 1$ ) for  $N = 100$  using DMRG. (a) Spin correlation function  $\langle S_1 S_1 \rangle$  for  $U = 2t$ . (b) Expectation value of  $S_1^z$  for  $U = 1$  in the sector  $S^z = S_g$ . Spin correlation function  $\langle S_{B1} S_{B1} \rangle$  for (c)  $U = 2t$  and (d)  $U = 1$ . (+) indicates odd (even) local parity. Dashed lines are guides to the eye. Illustration of the GS for (e)  $U = 1$  in the phase-separated regime and (f) at  $\beta = 1/3$ : singlet bonds are represented by ellipses and holes by circles.

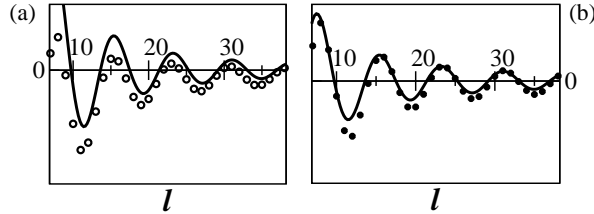


FIG. 11: Spin correlation functions  $C(l)$  for (a)  $U = 2t$  and (b)  $U = 1$  at  $\beta = 88=106$  for  $N = 106$  using DMRG: solid lines are fittings using Eq. (15).

#### IV. CONCLUSIONS

In this contribution on the celebration of the 80th birthday anniversary of Prof. Ricardo Ferreira, we have presented a brief review of the main experimental and theoretical achievements on quasi-one-dimensional magnetic compounds, featuring those with  $AB_2$  unit cell structure.

As reported, this has been an area of intense activity, particularly since the first experimental announcements in the mid 80's<sup>1,2,3,4</sup>. Nowadays several groups all over the world, involving chemists, physicists, and material scientists, are engaged in the characterization and description of properties of the already known materials, as well as doing great efforts towards the design and synthesis of new compounds, with novel properties suitable for technological applications<sup>80</sup>.

From the fundamental point of view, these compounds have been used as a laboratory in which many theoretical concepts and predictions in the field of low-dimensional materials have been tested.

In conclusion, it seems clear that this interdisciplinary research area will remain an exciting and topical one for many years to come, offering new challenges both from the scientific and technological aspects.

#### V. ACKNOWLEDGMENTS

We thank A. M. S. Macêdo, M. C. dos Santos, C. A. Macêdo and F. B. de Brito for collaboration in several stages of this research. Work supported by CNPq, CAPES, Finep and FACEPE (Brazilian agencies).

Electronic address: mdcff@ufpe.br

<sup>y</sup> Electronic address: rene@dfufpe.br

<sup>z</sup> Electronic address: emesto@dfufpe.br

<sup>x</sup> Electronic address: carlindovitoriano@ig.com.br

<sup>t</sup> Electronic address: mario@lftcufpe.br

<sup>1</sup> Y. V. Korshak, T. V. Medvedeva, A. A. Ovchinnikov, and V. N. Spector, *Nature* 326, 370 (1987); A. A. Ovchinnikov and V. N. Spector, *Synth. Met.* 27, B 615 (1988).

<sup>2</sup> M. Takahashi, P. Turek, Y. Nakazawa, M. Tamura, K. Nozawa, D. Shiomi, M. Ishikawa, and M. Kinoshita, *Phys. Rev. Lett.* 67, 746 (1991); M. Tamura, Y. Nakazawa, D.

Shiomi, K. Nozawa, Y. Hosokoshi, M. Ishikawa, M. Takahashi, and M. Kinoshita, *Chem. Phys. Lett.* 186, 401 (1991); Y. Nakazawa, M. Tamura, N. Shirakawa, D. Shiomi, M. Takahashi, M. Kinoshita, and M. Ishikawa, *Phys. Rev. B* 46, 8906 (1992).

<sup>3</sup> O. Kahn, *Molecular Magnetism* (VCH, New York, 1993); P. M. Lahti (ed.), *Magnetic Properties of Organic Materials* (Dekker, New York, 1999); see, also, J. S. Miller and A. J. Epstein, *Angew. Chem. Int. Ed. Engl.* 33, 385 (1994).

<sup>4</sup> J. S. Miller, P. J. K. Ruscic, A. J. Epstein, W. M. Rei, and J. H. Zhang, *Mol. Cryst. Liq. Cryst.* 120, 27 (1985); S.

- Chittipeddi, K. R. Cromack, J. S. Miller, and A. J. Epstein, *Phys. Rev. Lett.* **58**, 2695 (1987); J. S. Miller and A. J. Epstein, *Angew. Chem. Int. Ed. Engl.* **33**, 385 (1994); J. S. Miller and A. J. Epstein, *Chem. Commun.* **13**, 1319 (1998).
- <sup>5</sup> J. Silvestre and R. Hermann, *Inorg. Chem.* **24**, 4108 (1985).
- <sup>6</sup> H. Nishide, *Adv. Mater.* **7**, 937 (1995).
- <sup>7</sup> C. I. Ivanov, G. O. Ibrich, H. Barentzen, and O. E. Polansky, *Phys. Rev. B* **36**, 8712 (1987).
- <sup>8</sup> M. Yamada and M. Takahashi, *J. Phys. Soc. Japan* **54**, 2808 (1985); M. Takahashi, *Phys. Rev. Lett.* **58**, 168 (1997); P. Schlottmann, *Phys. Rev. Lett.* **54**, 2131 (1985); *Phys. Rev. B* **33**, 4880 (1986).
- <sup>9</sup> K. Yoshizawa, K. Tanaka, T. Yamabe, and J. Yamachi, *J. Chem. Phys.* **96**, 5516 (1992); M. Baumgarten, K. Mullen, N. Tyutyulkov, and G. M. Adjarova, *Chem. Phys.* **169**, 81 (1993); N. S. Sariciffci, A. J. Heeger, and Y. Cao, *Phys. Rev. B* **49**, 5988 (1994).
- <sup>10</sup> R. S. Kohlman, J. Joo, Y. Z. Wang, J. P. Pouget, H. Kaneko, T. Ishiguro, and A. J. Epstein, *Phys. Rev. Lett.* **74**, 773 (1995); K. Yoshioka, S. Masubuchi, S. Kazama, K. Mizoguchi, K. Kumae, H. Sakamoto, and N. Kachi, *Synth. Met.* **84**, 695 (1997). For related compounds, see: H. S. M. Lu and J. A. Berson, *J. Am. Chem. Soc.* **119**, 1428 (1997).
- <sup>11</sup> C. M. Wynn, M. A. G<sup>rtu</sup>, J. S. Miller and A. J. Epstein, *Phys. Rev. B* **56**, 14050 (1997); C. M. Wynn, M. A. G<sup>rtu</sup>, J. Zhang, J. S. Miller and A. J. Epstein, *Phys. Rev. B* **58**, 8508 (1998).
- <sup>12</sup> A. Caneschi, D. Gatteschi, J.-P. Renard, P. Rey, and R. Sessoli, *Inorg. Chem.* **28**, 1976 (1989); **28**, 2940 (1989); *J. Am. Chem. Soc.* **111**, 785 (1989).
- <sup>13</sup> M. D. Rillon, E. Coronado, M. Belache, and R. L. Carlin, *J. Appl. Phys.* **63**, 3551 (1988).
- <sup>14</sup> M. A. M. Abu-Youssef, A. Escuer, M. A. S. Goher, F. A. Mautner, G. J. Rei, and R. Vicente, *Angew. Chem., Int. Ed.* **39**, 1624 (2000).
- <sup>15</sup> E. Coronado, M. D. Rillon, A. Fuertes, D. Beltran, A. Mosset, and J. Galy, *J. Am. Chem. Soc.* **108**, 900 (1986).
- <sup>16</sup> E. Coronado, M. D. Rillon, P. R. Nugteren, L. J. de Jongh, and D. Beltran, *J. Am. Chem. Soc.* **110**, 3907 (1988).
- <sup>17</sup> A. Escuer, R. Vicente, M. S. E. Fallah, M. A. S. Goher, and F. A. Mautner, *Inorg. Chem.* **37**, 4466 (1998).
- <sup>18</sup> M. A. M. Abu-Youssef, M. D. Rillon, A. Escuer, M. A. S. Goher, F. A. Mautner, and R. Vicente, *Inorg. Chem.* **39**, 5022 (2000).
- <sup>19</sup> J. Cano, Y. Journaux, M. A. S. Goher, M. A. M. Abu-Youssef, F. A. Mautner, G. J. Rei, A. Escuer, and R. Vicente, *New J. Chem.* **29**, 306 (2005).
- <sup>20</sup> M. S. Reis, A. Moreira dos Santos, V. S. Amaral, P. Brandao, and J. Rocha, *Phys. Rev. B* **73**, 214415 (2006).
- <sup>21</sup> O. Kahn, Y. Pei, M. Verdager, J.-P. Renard, and J. Sletten, *J. Am. Chem. Soc.* **110**, 782 (1988).
- <sup>22</sup> P. J. van Koningsbruggen, O. Kahn, K. Nakatani, Y. Pei, and J.-P. Renard, *Inorg. Chem.* **29**, 3325 (1990).
- <sup>23</sup> M. Verdager, M. Julve, A. Michalowicz, and O. Kahn, *Inorg. Chem.* **22**, 2624 (1983); Y. Pei, M. Verdager, O. Kahn, J. Sletten, and J.-P. Renard, *ibid.* **26**, 138 (1987); P. J. van Koningsbruggen et al., *ibid.* **29**, 3325 (1990).
- <sup>24</sup> S. K. Pati, S. Ramasesha, and D. Sen, *Phys. Rev. B* **55**, 8894 (1997); S. Yamamoto, S. Brehm, and H.-J. Mikeska, *ibid.* **57**, 13610 (1998); N. B. Ivanov, *ibid.* **62**, 3271 (2000); S. Yamamoto, *ibid.* **69**, 064426 (2004), and references therein.
- <sup>25</sup> O. Kahn, E. Bakalbassis, C. Mathoniere, M. Hagiwara, K. Katsumata, and L. O. uahab, *Inorg. Chem.* **36**, 1530 (1997).
- <sup>26</sup> R. Clerac, H. Miyasaka, M. Yamashita, and C. Coulon, *J. Am. Chem. Soc.* **124**, 12837 (2002).
- <sup>27</sup> H. Iwamura, K. Inoue, and N. Koga, *New J. Chem.* **22**, 201 (1998).
- <sup>28</sup> A. S. Ovchinnikov, I. G. Bostren, V. E. Sinitsyn, N. V. Baranov, and K. Inoue, *J. Phys.: Condens. Matter* **13**, 5221 (2001).
- <sup>29</sup> A. S. Ovchinnikov, I. G. Bostren, V. E. Sinitsyn, A. S. Boyarchenkov, N. V. Baranov, and K. Inoue, *J. Phys.: Condens. Matter* **14**, 8067 (2002).
- <sup>30</sup> C. M. Wynn, M. A. G<sup>rtu</sup>, J. S. Miller and A. J. Epstein, *Phys. Rev. B* **56**, 315 (1997); C. M. Wynn, M. A. G<sup>rtu</sup>, K.-I. Sugiura, E. J. Brandon, J. L. Manson, J. S. Miller, and A. J. Epstein, *Synth. Met.* **85**, 1695 (1997); C. M. Wynn, M. A. G<sup>rtu</sup>, W. B. Brinckerhoff, K.-I. Sugiura, J. S. Miller, and A. J. Epstein, *Chem. Mater.* **9**, 2156 (1997); E. J. Brandon, A. M. Arif, B. M. Burkhardt, and J. S. Miller, *Inorg. Chem.* **37**, 2792 (1998); E. J. Brandon, D. K. Rittenberg, A. M. Arif, and J. S. Miller, *Inorg. Chem.* **37**, 3376 (1998).
- <sup>31</sup> K. Fegy, D. Luneau, E. Belbrizky, M. Novac, J.-L. Tholence, C. Paulsen, T. Ohm, and P. Rey, *Inorg. Chem.* **37**, 4524 (1998).
- <sup>32</sup> J. Seiden, *J. Phys. Lett.* **44**, 947 (1983).
- <sup>33</sup> J. B. Anderson, E. Kostiner, and F. A. Ruszala, *J. Solid State Chem.* **39**, 29 (1981).
- <sup>34</sup> M. D. Rillon, M. Belache, P. Legoll, J. Aride, A. Boukhari, and A. Moqine, *J. Magn. Magn. Mater.* **128**, 83 (1993).
- <sup>35</sup> A. A. Belik, A. Matsuo, M. Azuma, K. Kondo, and M. Takano, *J. Solid State Chem.* **178**, 709 (2005).
- <sup>36</sup> M. Matsuda, K. Kakurai, A. A. Belik, M. Azuma, M. Takano, and M. Fujita, *Phys. Rev. B* **71**, 144411 (2005).
- <sup>37</sup> A. Boukhari, A. Moqine, and S. Flandrois, *Mater. Res. Bull.* **21**, 395 (1986).
- <sup>38</sup> H. E. enberger, *J. Solid State Chem.* **142**, 6 (1999).
- <sup>39</sup> H. Kikuchi, Y. Fujii, M. Chiba, S. Mitsudo, T. Idehara, T. Tonegawa, K. Okamoto, T. Sakai, T. Kuwai, and H. Ohta, *Phys. Rev. Lett.* **94**, 227201 (2005).
- <sup>40</sup> K. Okamoto, T. Tonegawa, and M. Kaburagi, *J. Phys. Condens. Matter* **15**, 5979 (2003); H. H. Fu, K. L. Yao, and Z. L. Liu, *Phys. Rev. B* **73**, 104454 (2006); H. H. Fu, K. L. Yao, and Z. L. Liu, *Solid State Commun.* **139**, 289 (2006); B. Gu and G. Su, *Phys. Rev. B* **75**, 174437 (2007).
- <sup>41</sup> Y. Hosokoshi, K. Katoh, Y. Nakazawa, H. Nakano, and K. Inoue, *J. Am. Chem. Soc.* **123**, 7921 (2001); K. L. Yao, Q. M. Liu, and Z. L. Liu, *Phys. Rev. B* **70**, 224430 (2004); K. L. Yao, H. H. Fu, and Z. L. Liu, *Solid State Commun.* **135**, 197 (2005). See, also, the AB<sub>2</sub> quasi-1d compound Cu<sub>3</sub>(TeO<sub>3</sub>)<sub>2</sub>B<sub>2</sub>: D. Uematsu and M. Sato, *J. Phys. Soc. Jpn.* **76**, 084712 (2007).
- <sup>42</sup> E. H. Lieb, *Phys. Rev. Lett.* **62**, 1201 (1989); see, also, G.-S. Tian and T.-H. Lin, *Phys. Rev. B* **53**, 8196 (1996), for this special AB<sub>2</sub> topology.
- <sup>43</sup> A. M. S. M. acedo, M. C. dos Santos, M. D. Coutinho-Filho and C. A. M. acedo, *Phys. Rev. Lett.* **74**, 1851 (1995).
- <sup>44</sup> C. P. de Melo and S. A. F. Azevedo, *Phys. Rev. B* **53**, 16258 (1996).
- <sup>45</sup> Y. F. Duan and K. L. Yao, *Phys. Rev. B* **63**, 134434 (2001); W. Z. Wang, Bambi Hu, and K. L. Yao, *ibid.* **66**, 085101 (2002).
- <sup>46</sup> R. R. Montenegro-Filho and M. D. Coutinho-Filho, *Physica A* **357**, 173 (2005).

